Journal of Low Temperature Physics (2020) 199:789–797
https://doi.org/10.1007/s10909-019-02319-y

Developing a Large-Scale Cryogenic System for the Simultaneous Operation of Three Detector Focal Planes in TolTEC, A New Multichroic Imaging Polarimeter

N. S. DeNigris[1] · G. W. Wilson[1] · M. E. Eiben[1] · E. Lunde[2] · P. Mauskopf[2] · R. Contente[1]

Received: 21 August 2019 / Accepted: 17 December 2019 / Published online: 7 January 2020

Abstract

TolTEC is an upcoming millimeter-wave imaging polarimeter designed to fill the focal plane of the 50-m-diameter Large Millimeter Telescope (LMT). Combined with the LMT, TolTEC will offer high-angular-resolution (5″–10″) simultaneous, polarization-sensitive observations in three wavelength bands: 1.1, 1.4, and 2.0 mm. Additionally, TolTEC will feature mapping speeds greater than $2\,\mathrm{deg}^2/\mathrm{mJy}^2/\mathrm{h}$, thus enabling wider surveys of large-scale structure, galaxy evolution, and star formation. These improvements are only possible through the integration of approximately 7000 low-noise, high-responsivity superconducting Lumped Element Kinetic Inductance Detectors. Utilizing three focal planes of detector arrays requires the design, fabrication, and characterization of a unique, large-scale cryogenic system. Based on thermal models and expected photon loading, the focal planes must have a base operational temperature below 150 mK. To achieve this base temperature, TolTEC utilizes two cryocoolers, a Cryomech pulse tube cooler and an Oxford Instruments dilution refrigerator, to establish four thermal stages: 45 K, 4 K, 1 K, and 100 mK. During the design phase, we developed an object-oriented Python code to model the heat loading on each stage as well as the thermal gradients throughout the system. This model has allowed us to improve thermal gradients in the system as well as locate areas of poor thermal conductivity prior to ending a cooldown. The results of our model versus measurements from our cooldowns will be presented along with a detailed overview of TolTEC's cryogenic system. We anticipate TolTEC to be commissioned at the LMT by Spring 2020.

Keywords TolTEC · Cryogenics · KIDs

✉ N. S. DeNigris
ndenigris@umass.edu

[1] Department of Astronomy, University of Massachusetts, Amherst, MA 01002, USA

[2] School of Earth and Space Exploration, Arizona State University, Tempe, AZ 85281, USA

1 Introduction

While being on the cusp of a new Astronomy Decadal Survey, there is still a call for a fast, mm/submm wavelength telescope to conduct large-scale surveys of the mm-wavelength sky. TolTEC is a new multichroic imaging polarimeter designed to quickly and deeply map the mm-wavelength sky to meet these requirements [1–3]. The camera will be a facility instrument for the 50-m-diameter Large Millimeter Telescope (LMT) in Mexico. This being a follow-up to the AzTEC camera, which could only image in 1.1 mm, TolTEC will feature simultaneous imaging and polarimetry at 1.1 mm, 1.4 mm, and 2.0 mm with massive improvements to mapping speed [4]. Within the first decade of commissioning TolTEC, there will be ten 100-h public surveys, four of which have been defined in the last year to cover topics ranging from star formation to the evolution of large-scale structure (Table 1).

At the center of TolTEC are three focal plane arrays of about 7000 superconducting Lumped Element Kinetic Inductance Detectors (LEKIDs) [5–7]. The LEKIDs offer high sensitivity and intuitive multiplexing for high-density arrays. Based on thermal models and expected photon loading, the focal planes must have a base operational temperature between 100 and 150 mK, about ten times lower than the transition temperature of the focal plane, which have $T_C \approx 1.2$ K [1, 8]. For further details on the fabrication of the TolTEC detectors, see Austermann et al. [1].

In order to reach the desired base temperature, we have designed a unique, large-scale cryogenic system. This paper presents the design, fabrication, and characterization process for TolTEC's cryogenics. In designing this subsystem, we developed a generalizable Python library for thermal modeling. The design and workflow of the model are discussed in greater detail within Sect. 2. Section 3 explores test results during multiple cooldowns that have been used to characterize the system under different conditions. The paper concludes with a discussion of the timeline for completing TolTEC and the legacy surveys following the commissioning period.

2 Design

2.1 Thermal Stages

TolTEC's design, and consequentially large size, was driven by the 300-mm-diameter window and the area of the 4 K optics bench (1.3 m by 1.0 m). We required

Table 1 TolTEC specifications for the number of detectors, predicted angular resolution, and predicted mapping speed for each of the three bands

	1.1 mm	1.4 mm	2.0 mm	Units
Number of detectors	4012	1800	1172	
FWHM	5	6.3	9.5	arcsec
Mapping speed	1.9	3.1	10.5	$\mathrm{deg}^2/\mathrm{mJy}^2/\mathrm{hr}$

For a more detailed discussion on the optics design of TolTEC, see Bryan et al. [2]

this area in order to establish three individual focal planes. Ultimately, these features presented a unique challenge in developing a cryogenic system to handle the cooling on the physical scales dictated by the optics bench. We settled on a nested shell design (see Fig. 1) to facilitate modifications and repairs to the system by separating not only the cryogenics into separate parts, but also the electronic and optical subsystems. Thus, while each subsystem works in tandem, they reside in relative isolation for debugging and potential modification purposes.

As shown in Fig. 1, TolTEC is comprised of three modules: the main cryostat and its two cryocoolers. Interior to the room temperature outer vacuum shell (OVS), the camera features four thermal stages established by the cryocoolers: 45, 4, 1, and 0.1 K. We accomplish these four separate thermal stages through the use of support materials with low thermal conductances: G10 sheets and carbon fiber tubes.

As the first cryogenic stage, the 45 K stage shields the interior stages from stray IR photons and thermalizes the radio-frequency (RF) readout cables entering and leaving the cryostat from room temperature. Between the OVS and the 45 K shell are several layers of multilayer insulation (MLI). Additionally, the exterior of the 45 K stage was polished to a mirror finish in order to prevent the absorption of stray IR photons. Following several more layers of MLI, we arrive at the 4 K stage which contains the optics bench, the coax cables traveling from the 45 K stage to the detectors, and the low-noise amplifiers (LNAs) [3]. We use the 4 K stage as a heat sink for the RF chain and to reduce background optical loading on the detectors. The interior of the 4 K stage shell's lid has been covered

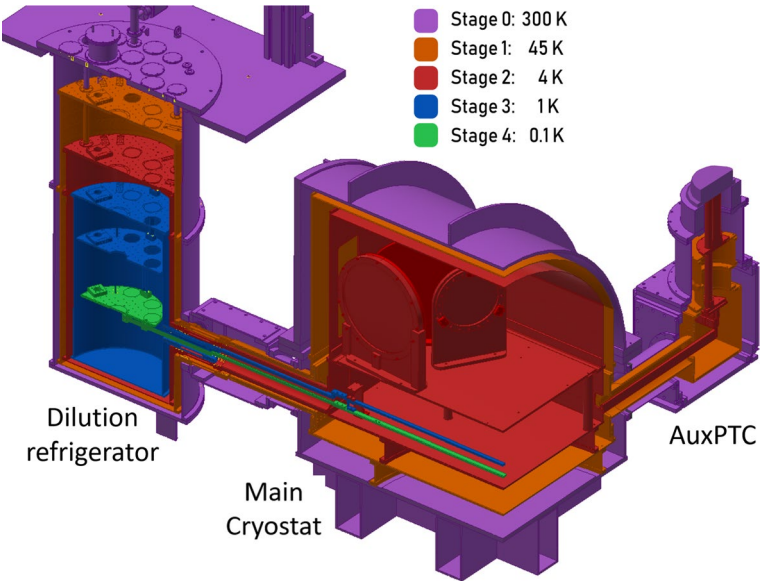

Fig. 1 CAD model of TolTEC, its four cryogenic stages, and its two cryocoolers. The two coolest stages reside below the optics bench in the 4 K volume, forming thermal links to the three detector focal planes. The unit on the left is the dilution refrigerator (DF), while the unit on the right is the auxiliary pulse tube cooler (AuxPTC) (Color figure online)

in reflective tape. Finally, the coldest two stages, 1 and 0.1 K, host the detector supports and the detector focal planes. The 1 K stage serves as an intermediate stage that heat-sinks the readout cabling attached to the detector array.

2.2 Cryocoolers

To cool the four different stages outlined above, we use two separate cryocooler systems. The first is a Cryomech 415 Pulse Tube Cooler, henceforth called the Auxiliary Pulse Tube Cooler (AuxPTC), which is coupled to the 45 and 4 K stages [9, 10]. In addition to the AuxPTC, we also use a custom-designed Oxford Instruments Triton 2016 dilution refrigerator (DF) to provide cooling at these two stages; however, the DF alone provides the heat lift for the two coldest stages [11].

The two warmer stages, 45 and 4 K, are established by bolted connections between oxygen-free high-conductivity copper (OFHC Cu) plates in the main cryostat shells to busbars (and cylinders) leading to cold heads/plates in the AuxPTC and DF. The two cooler stages, 1 and 0.1 K, are comprised of parallel sets of gold-plated OFHC Cu busbars traveling from the detector assemblies to the proper cold plates in the DF (see Figs. 2 and 3). Throughout all four thermal stages, we utilize custom-made copper straps to maintain high thermal conductance across joints. The straps also provide flexibility of joints during thermal contractions as well as vibration isolation from the cryocoolers.

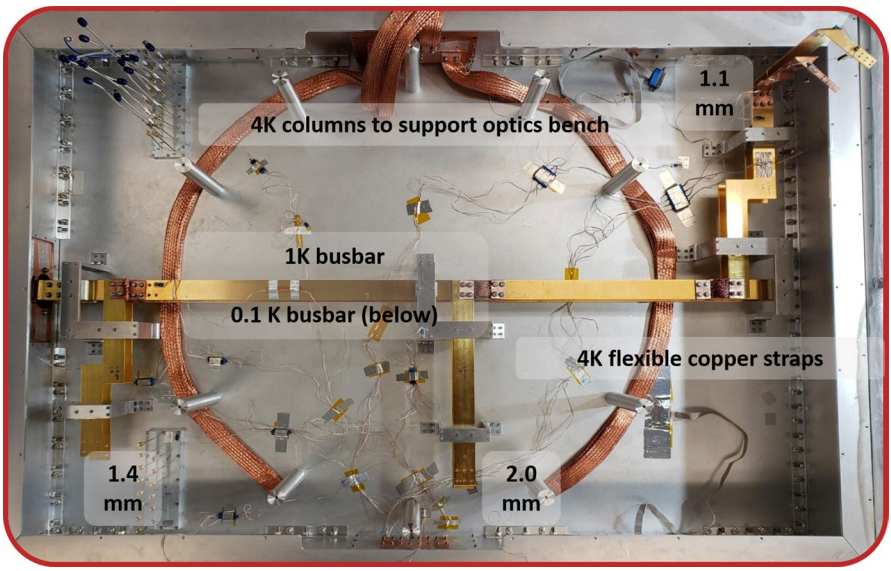

Fig. 2 Photograph of the interior of the 4 K volume below the optics bench showing the thermal busbar paths to the three focal planes (Color figure online)

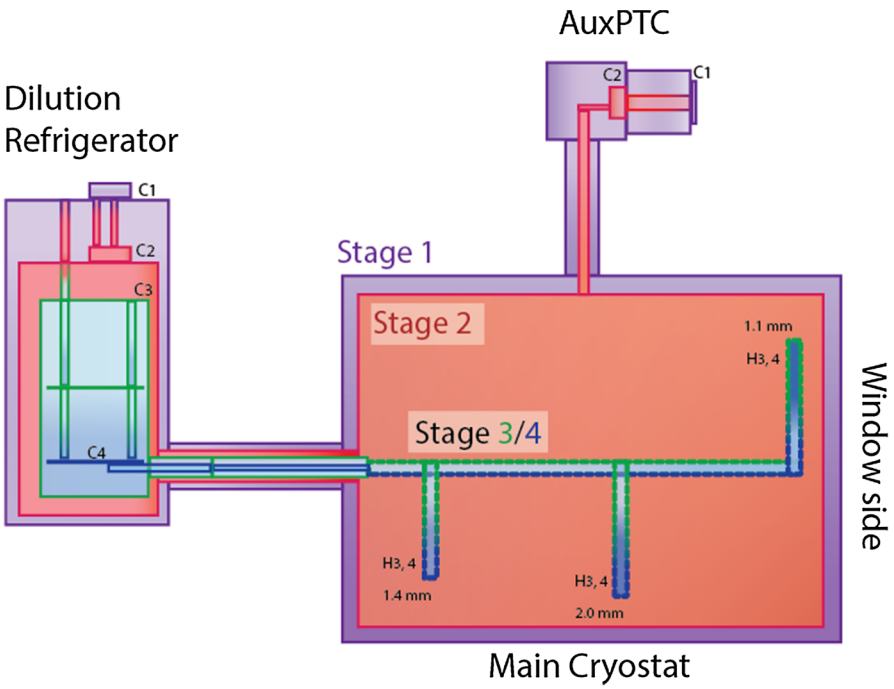

Fig. 3 Cartoon of the thermal gradients in the system with the stages drawn to scale. On the left in the dilution refrigerator, the locations of the cold heads are labeled C1, C2, C3, and C4; these correspond to the respective stage in Fig. 1. This is repeated on top with the AuxPTC where there are the two cold heads at 45 K (C1) and 4 K (C2). Within a given stage, darker colors hint at hotter temperatures. Stages 3 and 4 trace each other nearly perfectly and thus are shown as a single array of bars in the cartoon. Additionally, for Stages 3 and 4, the locations of the hot ends of the thermal busbars are made more explicit using the labels 'H3, 4' (Color figure online)

2.3 Thermal Model

The TolTEC thermal model was written in Python as a set of object-oriented libraries to be used in the design of a cryogenic system. It considers the four stages' temperatures and physical parameters such as the materials and geometric properties. The typical work flow of the model goes as this: use material properties and desired stage cold head temperatures to estimate the total heat loading on the system; use the estimated loading to then calculate thermal gradients in the system for given geometries and joints in each stage.

For the design of TolTEC, we developed two main libraries: a materials library with general physical properties and a stages library to model the four thermal stages. The first library includes materials common to a cryogenic system such as aluminum 6061 and OFHC Cu; however, it also contains properties of support materials such as G10 and carbon fiber, as well as characteristics of the stainless steel coax cables in our system. Each class in the materials library allows the user to set the cross-sectional area and length of the part and then calculates its mass, enthalpy,

and conductivity. To calculate the conductivities, we used the empirical equations determined by NIST for most materials between 300 and 4 K [12]. Below 4 K, we approximate the conductivity as a linear dependence on temperature when considering Al or OFHC Cu.

After generating the materials library, we developed Python classes to model each of the four stages. Within these stage classes, we consider the radiative and conductive loading on that stage assuming some cold head temperature. (In the case of the reported values, the assumed temperatures are 45, 4, 1, and 0.1 K.) For the radiative loading, we calculate the blackbody emission onto the stage from its warmer surroundings. The emissivity selected for this calculation is 10%, which is used as an upper limit for Stages 1 and 2's polished aluminum shells. As for the conductive loading, we include the heat from G10 and carbon fiber supports as well as power dissipated from the readout cabling. Additional sources of loading can easily be added to the stage classes by creating a function for each source of loading. For instance, at Stage 2, we heat-sink the LNAs used for detector readout; the LNAs generate $\sim$ 90 mW of conductive loading on the stage and require a bias current for power, which contributes additional conductive loading, on both Stages 1 and 2, through the wiring of the power supply external to the cryostat [3]. In Table 2, the modeled loading from the LNAs is included under the coax cables column for Stage 2.

Using the simple model outlined above, we were able to estimate the total radiative and conductive loading for each of TolTEC's four stages. Table 2 explores the results of the model compared to the measured loading and our cryocoolers' cooling power. One core assumption when applying the model for the first time is that the base temperatures that go into calculating the background radiation and thermal conductances are the desired stage temperatures. Subsequent applications of the model may utilize base temperatures as measured from the averages of prior cooldowns (see Table 3). Another key point is that the model assumes that all three detector arrays are installed with their readout cabling integrated. The loading from

Table 2 Modeled (for three detectors) and measured (with a single detector installed) heat loading and estimated cooling power

Stage (K)	Supports	Coax cables	Radiative loading	Total modeled loading (Col. 2 + 3 + 4)	Total measured loading for 1 array	Cooling power available
45	2.37 W	0.63 W	15.9 W	18.9 W	27.5 W	40 W (AuxPTC) + 10 W (DF)
4	0.16 W	0.25 W	0.02 W	0.43 W	1.25 W	1 W (AuxPTC) + 1 W (DF)
1	1.25 mW	1.16 mW	0.51 μW	2.41 mW	2.76 mW	$\leq$ 50 mW
0.1	37.7 μW	10.9 μW	0.51 μW	48.6 μW	14.9 μW	450 μW

For a given thermal stage, we use our thermal model to estimate the total heat load on the system through conduction from its mechanical supports (G10 and, for 1 and 0.1 K, G10 and carbon fiber), conduction from the coax cables, as well as through background radiation. The cooling powers from the AuxPTC and/or the DF are shown in the rightmost column. The reported DF cooling power values for each stage were characterized by Oxford Instruments

having three arrays only becomes a dominant factor when comparing the model to the measured values for Stage 4. With these assumptions, we were able to estimate the heat loading on the system to within a factor of three for all stages.

3 Characterization and Results

As of November 2019, we completed eleven cooldowns with all four thermal stages. In its August 2019 configuration, TolTEC performed tests using the 1.1 mm array including, but not limited to, microphonics and applied magnetic field testing. This past October, we integrated the 2.0 mm array and performed dark testing with two arrays installed. The system will be completed with the addition of the final detector array, 1.4 mm, in December 2019; however, all of the thermal connections required to integrate the existing system, and the new detectors have been installed and tested. As a note, the results reported only consider the thermal gradients in the system in the case where there was no optical loading (e.g., the detectors were not allowed to see out into the room).

In Table 3, we report the initial modeled temperature at the hottest location in a stage, assuming that the cold head of a stage is at 45, 4, 1, or 0.1 K. For Stages 1 and 2, this location is approximately on the lid of the shell. At Stages 3/4, the hottest location is at the 1.1 mm detector array, which is physically furthest from the DF heat sink. After performing our first cooldowns with the full system, we located additional hot spots on the front of the Stage 1/2 shells and, for Stage 2, around the edges of the optics bench. These have been tackled using our custom-made Cu straps to create thermal shorts between a hot region and respective plates on the 45/4 K shells that lead to either the AuxPTC or the DF.

Table 3 states the designed temperatures and the average base temperature for each stage across each cooldown. While the measured gradients are significantly higher than modeled, this can be traced back to either issues with modeling/fabricating the thermal links between the stages and the cryocoolers or poor heat sinking of thermometry. Most importantly, throughout this process, our thermal model was

Table 3 The mass of OFHC copper and aluminum 6061 in each thermal stage interior to the 300 K outer vacuum shield, as approximated using AutoCAD inventor

Stage	Mass (kg)	$T_{c,d}$ (K)	$T_{h,d}$ (K)	$T_{h,model}$	$T_{c,\,meas}$ (K)	$T_{h,\,meas}$ (K)
1	102.9	45	50	47.5	38.7	50.5
2	164.8	4	4.2	4.09	3.89	4.88
3	7.9	1	< 1.2	1.10	0.93	1.25
4	11.8	0.1	< 0.15	0.13	0.07	0.156

Here we also compare the design temperatures (subscript d) to the hot end model temperature and to the average measured temperature at each stage. While the ends of the stages tend to be hotter than designed, the average has been boosted by cooldown measurements with well-characterized issues that have been iteratively addressed

able to provide suggestions as to where we needed to improve these links while our thermometry data allowed us to tune our model.

4 Summary

TolTEC's high resolution is meant to pair well with observations from the next-generation observatories coming online within the next decade, allowing for new multi-wavelength studies. The design of TolTEC's cryogenic system was motivated by the required specifications for background loading on the detector focal planes, as well as by the physical size of the optics bench required for three focal planes operating simultaneously.

In order to facilitate the design and characterization of the system, we have built a simple, yet powerful Python toolbox for thermal modeling. While often the design of any cryogenic system for astronomy instrumentation will be a unique process, having a library to develop a model of the system can be generalized for other uses. Here we have highlighted the ability of our model to perform quick, yet intuitive estimates of thermal gradients within the system that can be used to diagnose issues with the cryostat design.

We completed the bulk of the cryogenic subsystem's development over the past year and a half. The results presented in this paper were produced with using the full integration between our two cryocoolers, the main cryostat, and one detector array between January and August 2019. We have achieved nominal base temperatures with a clear understanding of where to improve on thermal gradients in the system prior to shipment and commissioning of the camera. TolTEC will be installed at the LMT by February 2020 and will begin data collection over the following year.

Acknowledgements Thanks to the TolTEC team for their support and work on this project; this work could not be done without you. We sincerely thank H.D. Pinckney for suggestions on how to improve this manuscript. This project is generously funded by NSF Grant #1636621.

References

1. J.E. Austermann et al., *J. Low Temp. Phys.* (2018). https://doi.org/10.1007/s10909-018-1949-5. eprint: arXiv:1803.03280
2. S. Bryan et al., in *SPIE Conference Series*, vol. 10708 (2018). https://doi.org/10.1117/12.2314130. eprint: arXiv:1807.00097
3. M. Hosseini, W.T. Wong, J. Bardin, A 0.4–1.2 GHz SiGe cryogenic LNA for readout of MKID arrays, in *2019 IEEE/MTT-S International Microwave Symposium* (2019). http://par.nsf.gov/biblio/10112748
4. G.W. Wilson et al., in *The AzTEC mm-Wavelength Camera*, vol. 386, pp. 807–818 (2008). https://doi.org/10.1111/j.1365-2966.2008.12980.x. arXiv: 0801.2783
5. P.K. Day et al., in *Nature*, vol. 425, pp. 817–821 (2003). https://doi.org/10.1038/nature02037
6. J. Zmuidzinas, in *Annual Review of Condensed Matter Physics* (2012)
7. P. Mauskopf, in *Publications of the Astronomical Society of the Pacific* (2018)
8. H. McCarrick et al., in: 610, A45 (2018). https://doi.org/10.1051/0004-6361/201732044. eprint: arXiv:1710.02239

9. Pulse Tube Cooler 415 with Remote Motor. PT415-RM with CP1110. Cryomech (2007)
10. M.A. Green et al. Second stage cooling from a Cryomech PT415 cooler at second stage temperatures up to 300K with cooling on the first-stage from 0 to 250 W, in *IOP Conference Series: Materials Science and Engineering*, vol. 101, p. 012002 (2015). https://doi.org/10.1088/1757-899x/101/1/012002
11. G. Batey, A.J. Matthews, M. Patton, A new ultra-low-temperature cryogen-free experimental platform. J. Phys. Conf. Ser. **568**(3) 032014 (2014). https://doi.org/10.1088/1742-6596/568/3/032014
12. E. Marquardt, J. Le, R. Radebaugh, in *Cryogenic Material Properties Database*, pp. 681–687 (2002). https://doi.org/10.1007/0-306-47112-4_84